Autophagy Facilitates *Salmonella* Replication in HeLa Cells

Hong B. Yu,[a] Matthew A. Croxen,[a] Amanda M. Marchiando,[b,c] Rosana B. R. Ferreira,[a] Ken Cadwell,[b,c] Leonard J. Foster,[d] B. Brett Finlay[a]

Centre for High-Throughput Biology and Department of Biochemistry, University of British Columbia, Vancouver, British Columbia, Canada[a]; Department of Microbiology, New York University School of Medicine, New York, New York, USA[b]; Kimmel Center for Biology and Medicine at the Skirball Institute, New York University School of Medicine, New York, New York, USA[c]; Michael Smith Laboratories, University of British Columbia, Vancouver, British Columbia, Canada[d]

ABSTRACT **Autophagy is a process whereby a double-membrane structure (autophagosome) engulfs unnecessary cytosolic proteins, organelles, and invading pathogens and delivers them to the lysosome for degradation. We examined the fate of cytosolic *Salmonella* targeted by autophagy and found that autophagy-targeted *Salmonella* present in the cytosol of HeLa cells correlates with intracellular bacterial replication. Real-time analyses revealed that a subset of cytosolic *Salmonella* extensively associates with autophagy components p62 and/or LC3 and replicates quickly, whereas intravacuolar *Salmonella* shows no or very limited association with p62 or LC3 and replicates much more slowly. Replication of cytosolic *Salmonella* in HeLa cells is significantly decreased when autophagy components are depleted. Eventually, hyperreplication of cytosolic *Salmonella* potentiates cell detachment, facilitating the dissemination of *Salmonella* to neighboring cells. We propose that *Salmonella* benefits from autophagy for its cytosolic replication in HeLa cells.**

IMPORTANCE **As a host defense system, autophagy is known to target a population of *Salmonella* for degradation and hence restricting *Salmonella* replication. In contrast to this concept, a recent report showed that knockdown of Rab1, a GTPase required for autophagy of *Salmonella*, decreases *Salmonella* replication in HeLa cells. Here, we have reexamined the fate of *Salmonella* targeted by autophagy by various cell biology-based assays. We found that the association of autophagy components with cytosolic *Salmonella* increases shortly after initiation of intracellular bacterial replication. Furthermore, through a live-cell imaging method, a subset of cytosolic *Salmonella* was found to be extensively associated with autophagy components p62 and/or LC3, and they replicated quickly. Most importantly, depletion of autophagy components significantly reduced the replication of cytosolic *Salmonella* in HeLa cells. Hence, in contrast to previous reports, we propose that autophagy facilitates *Salmonella* replication in the cytosol of HeLa cells.**

Received 27 January 2014 **Accepted** 12 February 2014 **Published** 11 March 2014

Citation Yu HB, Croxen MA, Marchiando AM, Ferreira RBR, Cadwell K, Foster LJ, Finlay BB. 2014. Autophagy facilitates *Salmonella* replication in HeLa cells. mBio 5(2):e00865-14. doi:10.1128/mBio.00865-14.

Editor Arturo Zychlinsky, Max Planck Institute for Infection Biology

Address correspondence to B. Brett Finlay, bfinlay@interchange.ubc.ca.

Salmonella enterica serovar Typhimurium is a facultative intracellular pathogen that causes diseases ranging from self-limited gastroenteritis to typhoid fever in humans and mice (1). It contains two type III secretion systems (T3SSs) encoded by *Salmonella* pathogenicity island 1 (SPI-1) and SPI-2. These T3SSs are necessary for *Salmonella* pathogenicity and deliver bacterial proteins (effectors) to the host cell cytosol to manipulate host cell signaling, cytoskeletal, and vesicular pathways (2). In mouse infection models, *Salmonella* can enter specialized intestinal epithelial microfold (M) cells and gallbladder epithelial cells, and both epithelial cell types play important roles in the establishment of *Salmonella* infection (3, 4). To better understand the mechanisms of *Salmonella* interactions with epithelial cells, various tissue culture epithelial cell lines have been widely used, including HeLa, Henle 407, and Caco2 epithelial cells (2, 5). Upon invasion into mammalian cells, most *Salmonella* bacteria remain in a single membrane-bounded compartment called the *Salmonella*-containing vacuole (SCV). The SCV rapidly acquires late endosomal markers, such as the lysosomal-associated membrane protein 1 (LAMP-1). Although the SCV appears to be the default niche where *Salmonella* resides, some bacteria escape from the SCV and replicate rapidly in the host cell cytosol (6). However, the mechanism underlying this phenotype remains unclear. It was recently shown that hyperreplicating cytosolic bacteria (defined as >50 bacteria per cell; the doubling time of these bacteria is around 20 min) present in epithelial cells express SPI-1 genes and possess flagella, both of which prime *Salmonella* for further invasion (5). These invasion-primed *Salmonella* bacteria are released into the lumen through extrusion of epithelial cells that contain hyperreplicating bacteria, initiating secondary infections in neighboring cells, indicating that invasive *Salmonella* can disseminate through bacterium-induced extrusion of mucosal epithelia.

Many unnecessary cellular components or invading pathogens can be engulfed by a double-membrane structure (autophagosome) and delivered to the lysosome for degradation (7). This process is called autophagy. Various host components are involved in the autophagy pathway, such as LC3, Atg5, and p62. LC3 is present in two forms, cytosolic LC3-I and autophagosome-

associated LC3-II that is converted from a fraction of LC3-I (8). The levels of LC3-II correlate with autophagosome formation, and green fluorescent protein (GFP)-LC3 is therefore traditionally used as a marker for the autophagosomes (8). Atg5, through association with Atg12 to form a conjugation complex, mediates the conjugation of LC3 to autophagosomes (9). p62 (also called sequestosome 1) interacts with LC3 and ubiquitin that usually serves as a molecular tag for protein aggregates, thus functioning as an adaptor protein to target proteins to autophagosomes (7, 10). Many pathogens can be targeted by autophagy in the cytosol. Some pathogens (group A *Streptococcus* and *Mycobacterium tuberculosis*) can be killed by autophagy, while others (*Shigella flexneri*, *Listeria monocytogenes*, and *Yersinia pseudotuberculosis*) are able to antagonize the autophagy pathway or exploit autophagosomes for their benefit.

Salmonella can damage the SCV through SPI-1 components (11). It has been suggested that autophagy targets a population of *Salmonella* found in damaged SCVs or in the cytosol for degradation and hence restricts *Salmonella* replication. Paradoxically, a recent report showed that knockdown of Rab1, a GTPase required for autophagy of *Salmonella*, decreases *Salmonella* replication in HeLa cells (12). These contradictory results prompted us to reexamine the interaction of autophagy with *Salmonella* and track the fate of *Salmonella* targeted by autophagy by a live-cell imaging method. Contrary to previous reports, we showed that autophagy facilitates *Salmonella* replication in the cytosol of epithelial cells.

RESULTS

The association of p62 and/or LC3 with cytosolic *Salmonella* increases shortly after initiation of intracellular replication. Like many other groups who have used HeLa cells to study the interaction of *Salmonella* with autophagy (13–16), we created HeLa cell lines stably expressing GFP-p62 or GFP-LC3 and infected them with *Salmonella*. *Salmonella* replicates in the SCV and the cytosol in epithelial cells, but its cytosolic replication accounts for the majority of its net replication (17). We aimed to determine the percentage of autophagy (p62 or LC3)-targeted *Salmonella* that is present in the cytosol over time and see how it correlates with intracellular *Salmonella* replication.

Both wild-type (WT) and Δ*sifA Salmonella* strains were used to infect HeLa cells, as the Δ*sifA* strain (compared to the WT) escapes more frequently from the SCV into the cytosol, where it is more likely to be targeted by autophagy (15, 18). The association of p62 and LC3 with both *Salmonella* strains was measured at 1, 5, and 8 h postinfection (hpi). As shown in Fig. 1A, a subpopulation of *Salmonella* was associated with GFP-p62 ($p62^+$) but not GFP alone. The percentage of $p62^+$ *Salmonella* gradually decreased over time (from 1 hpi to 8 hpi) (Fig. 1B), consistent with the previous report where the association of endogenous p62 with *Salmonella* has been examined (19).

We then determined the intracellular location of $p62^+$ *Salmonella* by examining the colocalization of these bacteria with LAMP-1, a marker for the SCV membrane (6). As shown in Fig. 1C, the percentage of LAMP-1^- $p62^+$ bacteria (cytosolic) out of total $p62^+$ *Salmonella* increased from ~15% (WT) and ~22% (Δ*sifA* strain) at 1 hpi to ~42% (WT) and ~52% (Δ*sifA* strain) at 5 hpi. The presence of cytosolic $p62^+$ *Salmonella* was confirmed by immunostaining for ubiquitin, a marker for *Salmonella* present in the host cell cytosol (20) (see Fig. S1A in the supplemental material). Since it is known that *Salmonella* replication in epithelial cells commences at 4.5 to 6 hpi (21), we conclude that the increased presence of cytosolic $p62^+$ *Salmonella* at 5 hpi correlates with intracellular replication of *Salmonella*. It appears that such an increased presence of cytosolic $p62^+$ *Salmonella* is proportional to the increased presence of cytosolic bacteria in the total *Salmonella* population (from 1 hpi to 5 hpi) (Fig. 1D). In line with this, the Δ*sifA* strain that showed a slightly higher (although insignificantly) percentage of LAMP-1^- bacteria than the WT at 5 hpi had a higher percentage of cytosolic $p62^+$ bacteria (Fig. 1B to D). Interestingly, although the percentage of $p62^+$ *Salmonella* decreased significantly from 5 hpi to 8 hpi, the percentage of LAMP-1^- $p62^+$ *Salmonella* and the percentage of LAMP-1^- *Salmonella* did not change significantly between these two time points (Fig. 1C and D).

LC3 associated with *Salmonella* (WT and Δ*sifA* strains) in a manner that mimicked p62-*Salmonella* association (see Fig. S1A to D in the supplemental material). Most *Salmonella*-associated LC3 signals represent autophagosome structures (see Fig. S1E), since the association of LC3 with *Salmonella* ($LC3^+$ *Salmonella*) is dependent on Atg5, a protein required for autophagosome formation (9). An electron microscopy study suggested that autophagosome structures were associated with *Salmonella* that is present in the cytosol (the bacterium indicated by the black arrowhead in Fig. S1F to Fiii) or partially exposed to the cytosol (bacteria indicated by black arrowheads in Fig. S1Fi) through damaged SCVs, consistent with previous reports (15, 16). The association of LC3 with *Salmonella* also requires p62, since cells treated with p62 small interfering RNA (siRNA) showed decreased colocalization of LC3 with *Salmonella* (see Fig. S1E). In support of this result, p62 and LC3 colocalized extensively, targeting the same bacterium (see Fig. S1G and H). This is also consistent with the previous report where the association of endogenous p62 with transiently expressed LC3 has been examined (19).

Collectively, these results not only confirm that p62 and LC3 participate in the autophagy pathway and associate with *Salmonella* but also suggest that the association of p62 and/or LC3 with cytosolic *Salmonella* correlates with *Salmonella* replication.

Dynamic association of p62 and/or LC3 correlates with *Salmonella* replication in the cytosol of HeLa cells. To further probe this area, we examined the fate of *Salmonella* associated with p62 and/or LC3 by a live-cell imaging analysis method.

First, GFP-LC3-expressing HeLa cells were infected with monomeric Kusabira orange fluorescent (mKO)-expressing WT *Salmonella* (WT-mKO). As shown in Fig. 2A and Movie S1 in the supplemental material, LC3 associated with *Salmonella* (GFP-$LC3^+$) in multiple patterns. In one case, GFP-LC3 puncta (Fig. 2A, arrowhead labeled "2") gradually expanded and associated with *Salmonella* from two poles of the same bacterium or one pole of each dividing bacterium. These puncta then transiently fused with each other, completely surrounding the bacterium. In less than 30 min, they disappeared from one pole, accompanied by the completion of cell division of this bacterium. In other cases, GFP-LC3 puncta associated with *Salmonella* at one side or one pole of the bacterium (Fig. 2A, arrowheads labeled "1" and "3"). Overall, GFP-LC3 puncta moved rapidly in the cell and appeared to transiently associate with *Salmonella*, highlighting the dynamic association of LC3 with *Salmonella*. Some bacteria, appearing in light red (e.g., arrowheads labeled "1," "2," and "3"), associated with GFP-LC3 extensively and replicated in less than 30 minutes, as shown previously for hyperreplicating cytosolic bacteria (5). In

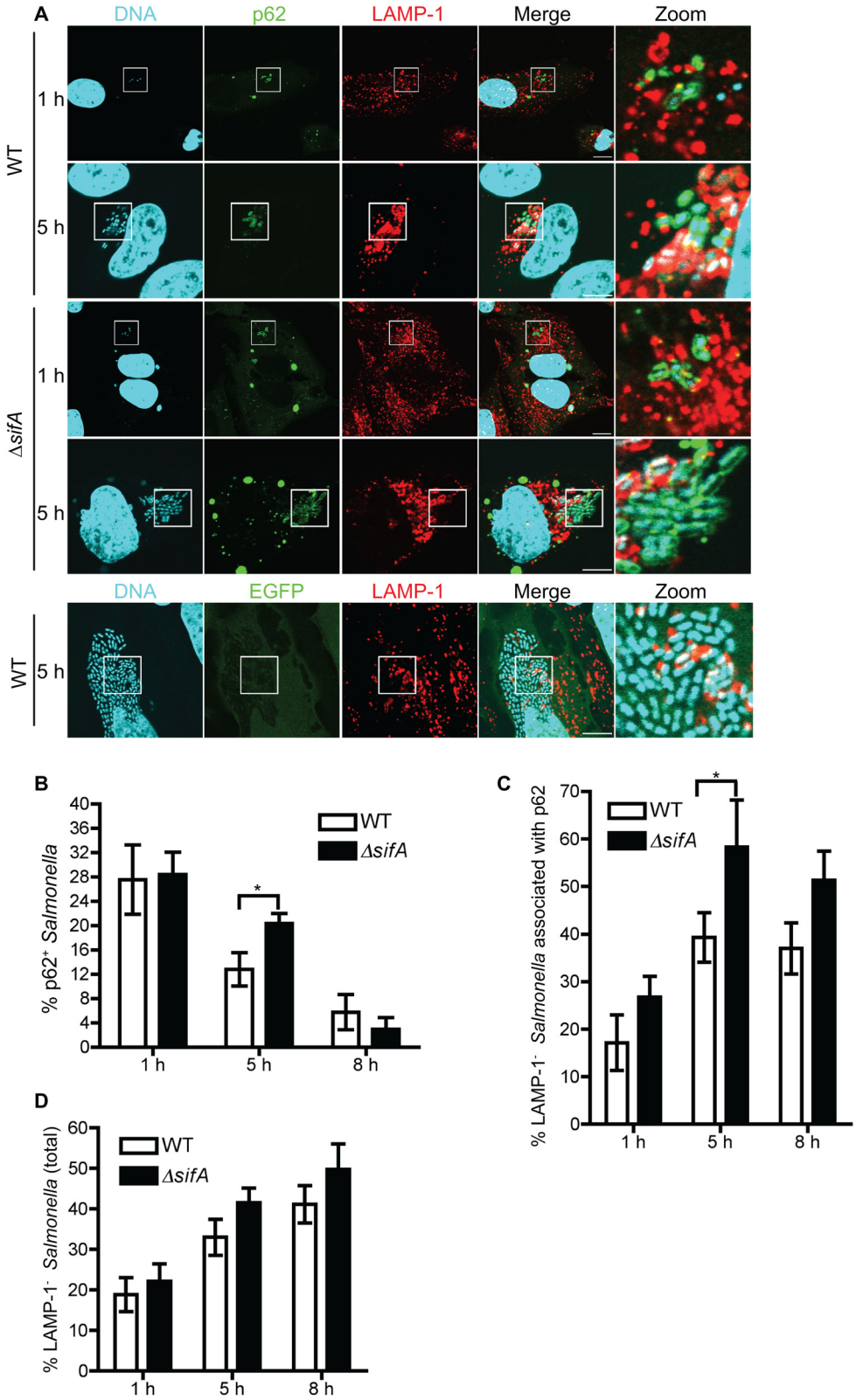

FIG 1 The association of p62 with cytosolic *Salmonella* increases shortly after initiation of intracellular replication. (A) GFP-p62- or GFP-expressing HeLa cells were infected with wild-type (WT) or Δ*sifA Salmonella*. Cells at 1 hpi and 5 hpi were stained with LAMP-1 (red) and DAPI (cyan). "Zoom" represents a magnified picture of the boxed area. Scale bar, 10 μm. (B to D) Quantification of the percentage of p62$^+$ WT or p62$^+$ Δ*sifA* bacteria (B), the percentage of p62$^+$ WT or p62$^+$ Δ*sifA* bacteria that are not associated with LAMP-1 (C), and the percentage of LAMP-1$^-$ WT or LAMP-1$^-$ Δ*sifA* bacteria (D) in GFP-p62-expressing cells at 1, 5, and 8 hpi (mean ± SD, $n = 3$).

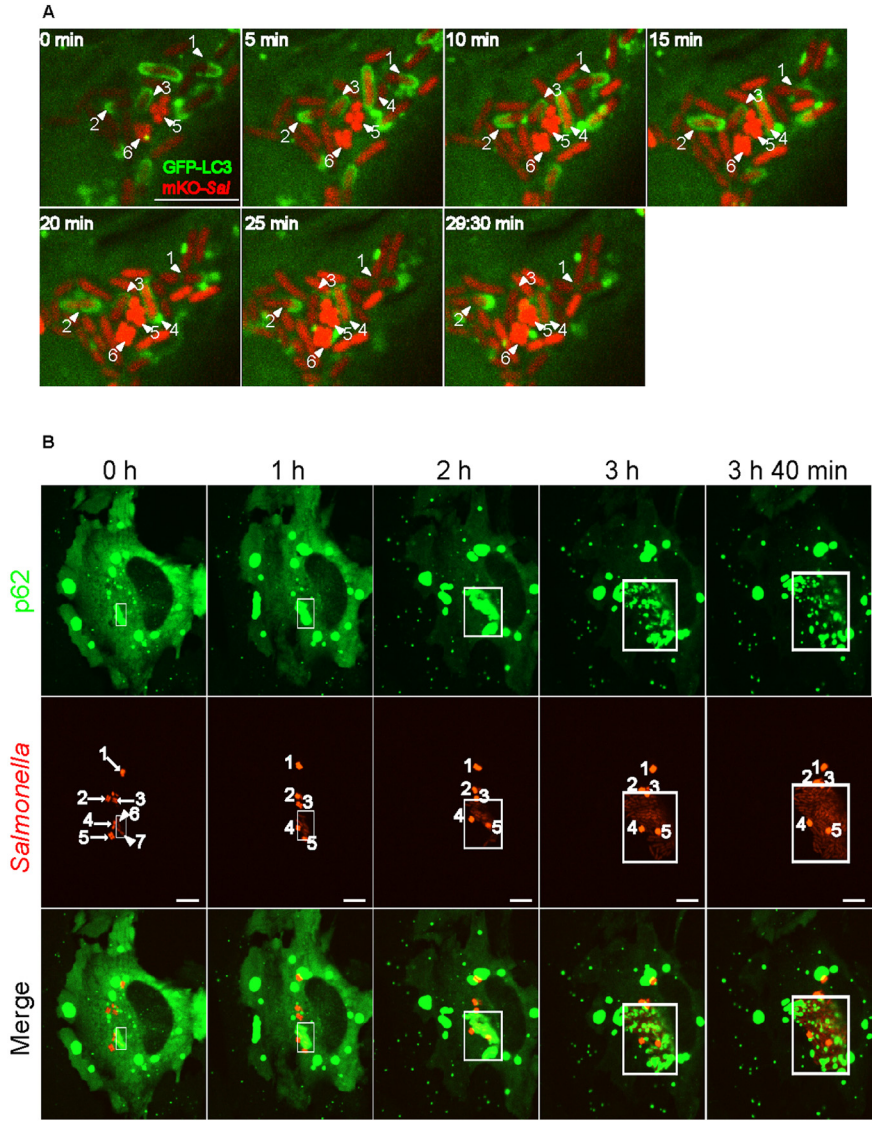

FIG 2 Dynamic association of p62 and/or LC3 correlates with *Salmonella* replication in the cytosol of HeLa cells. (A) GFP-LC3-expressing cells were infected with mKO-expressing *Salmonella*. After infection for 4.5 h (0 min), cells were imaged at 30-s intervals with a spinning-disc confocal microscope. A series of live-cell imaging data is shown, and the elapsed time (minutes) is shown in the corner of each picture. Arrowheads 1, 2, 3, and 4 indicate replicating bacteria, whereas arrowheads 5 and 6 indicate nonreplicating bacteria. Scale bar, 10 μm. (B) GFP-p62-expressing cells were infected with mKO-expressing *Salmonella*. After infection for 4.5 h (0 h), the cells were imaged at 20-s intervals with a spinning-disc confocal microscope. Boxed areas indicate where p62 associates with cytosolic *Salmonella*. Arrows 1 to 5 indicate bright bacteria that are not replicating; arrowheads 6 and 7 in column 1 (0 h) indicate light-red bacteria that start to replicate. Scale bar, 5 μm.

contrast, other bacteria, appearing in bright red (arrowheads labeled "5" and "6"), did not associate with GFP-LC3 and were not replicating; these bacteria are likely in SCVs. LAMP-1 staining of *Salmonella*-infected cells suggested the light-red GFP-LC3$^+$ bacteria represent *Salmonella* present in damaged SCVs or in the cytosol of host cells, whereas the bright-red GFP-LC3$^-$ bacteria represent *Salmonella* in intact SCVs (see Fig. S2A). Real-time analysis of GFP-LC3-expressing cells infected with wild-type cyan fluorescent protein (CFP)-expressing *Salmonella* (WT-CFP) in the presence of LysoTracker (which labels acidic compartments, including the SCV) also showed that GFP-LC3$^+$ *Salmonella* was not in an intact SCV (see Movie S2).

Next, GFP-p62-expressing cells were infected with WT-mKO. During 4 h of real-time imaging, a subset of cytosolic *Salmonella* associated with p62 extensively and replicating rapidly (Fig. 2B, bacteria in light red in boxed areas; see also Movie S3). In contrast to p62$^+$ bacteria, most *Salmonella* bacteria in intact SCVs (bright red) showed very limited association with p62 (Fig. 2B, bacteria labeled by arrows 2 to 5; see also Movie S3). These bacteria were not replicating.

Last, cells expressing GFP-p62 and mRFP-LC3 were infected with WT-CFP. The same bacterium clearly associated with both p62 and LC3 and was replicating in less than 30 min (see Fig. S2B, bacteria indicated by white arrows, and Movie S4). Many mRFP-LC3 puncta frequently and rapidly moved along the surface of *Salmonella* bacteria, with GFP-p62 signals being redistributed to

dividing bacteria. Future work is to determine if/how the redistribution of p62 affects the traffic pattern of LC3 (autophagosomes) to the surface of *Salmonella* bacteria.

Overall, live-cell imaging analysis demonstrates that a subpopulation of *Salmonella* is dynamically associated with p62 and LC3 while replicating in the cytosol of epithelial cells.

p62 and autophagy support *Salmonella* replication in the cytosol of HeLa cells. To investigate whether *Salmonella* benefits from p62 and LC3 for its replication in the cytosol, we determined if depletion of autophagy proteins by siRNA would decrease the cytosolic replication of *Salmonella*, using a gentamicin protection assay and a microscopic analysis that quantifies the percentage of infected cells containing different numbers of bacteria per cell.

The replication of WT *Salmonella* in HeLa cells treated with control siRNA or siRNA targeting p62, LC3 (including isoforms LC3A, LC3B, and LC3C) (22), Atg5, or p62 and LC3 was first determined. Western blot analysis confirmed that LC3, Atg5, and p62 were effectively knocked down in cells treated with corresponding siRNA (Fig. 3A). Knockdown of LC3, Atg5, or p62 and LC3 by siRNA significantly decreased autophagy, as evidenced by the decreased levels of LC3-II (Fig. 3A). In contrast, knockdown of p62 did not affect autophagy, as the level of LC3-II remained similar in control siRNA- and p62-siRNA-treated cells. Knockdown of p62, LC3, Atg5, or p62 plus LC3 did not affect the invasion ability of *Salmonella*, as assessed by the population of infected cells containing different numbers of bacteria at 2 hpi (Fig. 3B, top). However, the replication of *Salmonella* in cells treated with p62, LC3, Atg5, or p62 and LC3 siRNA was significantly reduced compared to that in cells treated with control siRNA at 6 and 8 hpi (Fig. 3C). Knockdown of Atg16L1, another subunit of the large protein complex containing the Atg5-Atg12 conjugate (23), decreased *Salmonella* replication to a similar extent as knockdown of Atg5 (see Fig. S3A and B). The decreased replication of *Salmonella* in cells treated with p62, LC3, Atg5, or p62 and LC3 siRNA was not due to detachment of infected cells from plates at 6 hpi, as all cells showed similar cell viability (see Fig. S3C). The knockdown of p62 and LC3 did not have an additive effect on the replication of *Salmonella* compared to the knockdown of p62 or LC3 alone (Fig. 3A), indicating that p62 and LC3 are involved in the same pathway that facilitates *Salmonella* replication. Additionally, control siRNA-treated cells showed a greater percentage of cells with high numbers of bacteria than autophagy protein siRNA-treated cells at 6 hpi, concomitant with a decreased percentage of cells with low numbers of bacteria (Fig. 3B, bottom). At 8 hpi, a decrease in the bacterial replication was observed, suggesting that some of the infected cells may have detached from plates.

As discussed above, a larger fraction of Δ*sifA* bacteria (compared to WT bacteria) was present in the cytosol and associated with LC3. As expected, Δ*sifA* bacteria exhibited the same replication defect as WT *Salmonella* in LC3 siRNA-treated cells (see Fig. S3D and E).

TBK1 helps to maintain the integrity of vacuolar membranes during intracellular bacterial infection, and knockdown of TBK1 leads to the disruption of SCVs, resulting in release of *Salmonella* into the host cell cytosol, where *Salmonella* hyperreplicates (24). GFP-LC3-expressing and regular HeLa cells were treated with siRNA that targets TBK1, TBK1 and LC3 (TBK1-LC3), or TBK1 and Atg5 (TBK1-Atg5), followed by infection with *Salmonella*. Consistent with the previous report (24), TBK1 siRNA-treated cells showed a higher percentage of LAMP-1$^-$ *Salmonella* at 5 hpi and had a significantly higher percentage of cells containing more than 20 bacteria than control siRNA-treated cells at 6 hpi (Fig. 3D, bottom; Fig. 3E, right). Furthermore, TBK1 siRNA-treated cells showed a slightly but insignificantly higher percentage of LC3$^+$ *Salmonella* bacteria than control siRNA-treated cells (Fig. 3E, left). However, the percentage of LC3$^+$ bacteria dropped dramatically when cells depleted of TBK1 were further treated with LC3 siRNA or Atg5 siRNA; this correlated with a significant decrease in the percentage of cytosolic bacteria (LAMP-1$^-$) and cells containing more than 20 bacteria in TBK1-LC3 siRNA- or TBK1-Atg5 siRNA-treated cells (compared to TBK1 siRNA-treated cells) at late time points (Fig. 3D, bottom; Fig. 3E, right). These differences were not caused by a different invasion rate of *Salmonella* to cells, as the numbers of intracellular bacteria at 2 hpi are similar among different siRNA-treated cells (Fig. 3D, top). The knockdown efficiency of each protein was confirmed by Western blotting (Fig. 3F). Thus, knockdown of autophagy components decreases the hyperreplication of cytosolic *Salmonella* in TBK1 siRNA-treated cells.

Taken together, these results demonstrate that p62 and autophagy support *Salmonella* replication in the cytosol of HeLa cells.

The effector SopB is required for *Salmonella* to associate with autophagosomes. It has been shown that *Salmonella* autophagy requires the SPI-1 T3SS (16). As multiple effectors are translocated via the SPI-1 T3SS, we attempted to determine which effector(s) could increase the association of autophagosomes with *Salmonella* and thus promote *Salmonella* replication in HeLa cells.

First, we examined the colocalization of LC3 with the WT and several *Salmonella* mutants (the Δ*invA*, Δ*sopB*, Δ*sopE* Δ*sopE2*, Δ*sptP*, Δ*sipA*, Δ*sipB*, and Δ*ssaR* mutants). The Δ*invA* (*invA* encodes an inner membrane protein) and Δ*sipB* mutants do not translocate any SPI-1 effectors (including SipB itself) (25), whereas the Δ*ssaR* mutant does not translocate any SPI-2 effectors into host cells (26). Δ*invA* bacteria barely associated with LC3, while Δ*ssaR* bacteria associated with LC3 to the same extent as the WT (16). These two mutants were used as controls. The remaining mutants lack one or two SPI-1 effectors that can promote *Salmonella* replication rate or invasion ability (27, 28). Unlike other mutants, Δ*invA* and Δ*sipB* bacteria are unable to invade into epithelial cells (data not shown) and therefore are used in a coinfection model as described previously (21). It is believed coinfection of cells with WT and Δ*invA* (or Δ*sipB*) bacteria facilitates the SPI-1-dependent cointernalization of Δ*invA* (or Δ*sipB*) bacteria with the WT. As shown in Fig. 4A, Δ*sipB* and Δ*invA* mutants had little association with LC3, whereas Δ*sopE* Δ*sopE2*, Δ*sptP*, Δ*sipA*, Δ*ssaR*, and WT strains were associated with LC3 at similar levels. Δ*sopB* bacteria were also able to associate with LC3, albeit less frequently than the WT. The decreased association of LC3 with Δ*sopB* could be rescued by overexpression of SopB in the Δ*sopB* mutant (Δ*sopB*/pACDE mutant).

Next, the replication of the above-described mutants, except the Δ*sipB* mutant in control siRNA- and LC3 siRNA-treated cells, was measured. We reasoned that if a mutant showed low (compared to that of the WT) or no association with autophagosomes, its replication would be independent of autophagy. Western blot analysis confirmed that LC3 was effectively depleted by siRNA treatment (Fig. 4B). As shown in Fig. 4C, LC3 siRNA treatment compared to control siRNA treatment decreased the replication of all mutants except the Δ*invA* mutant, although the decrease for

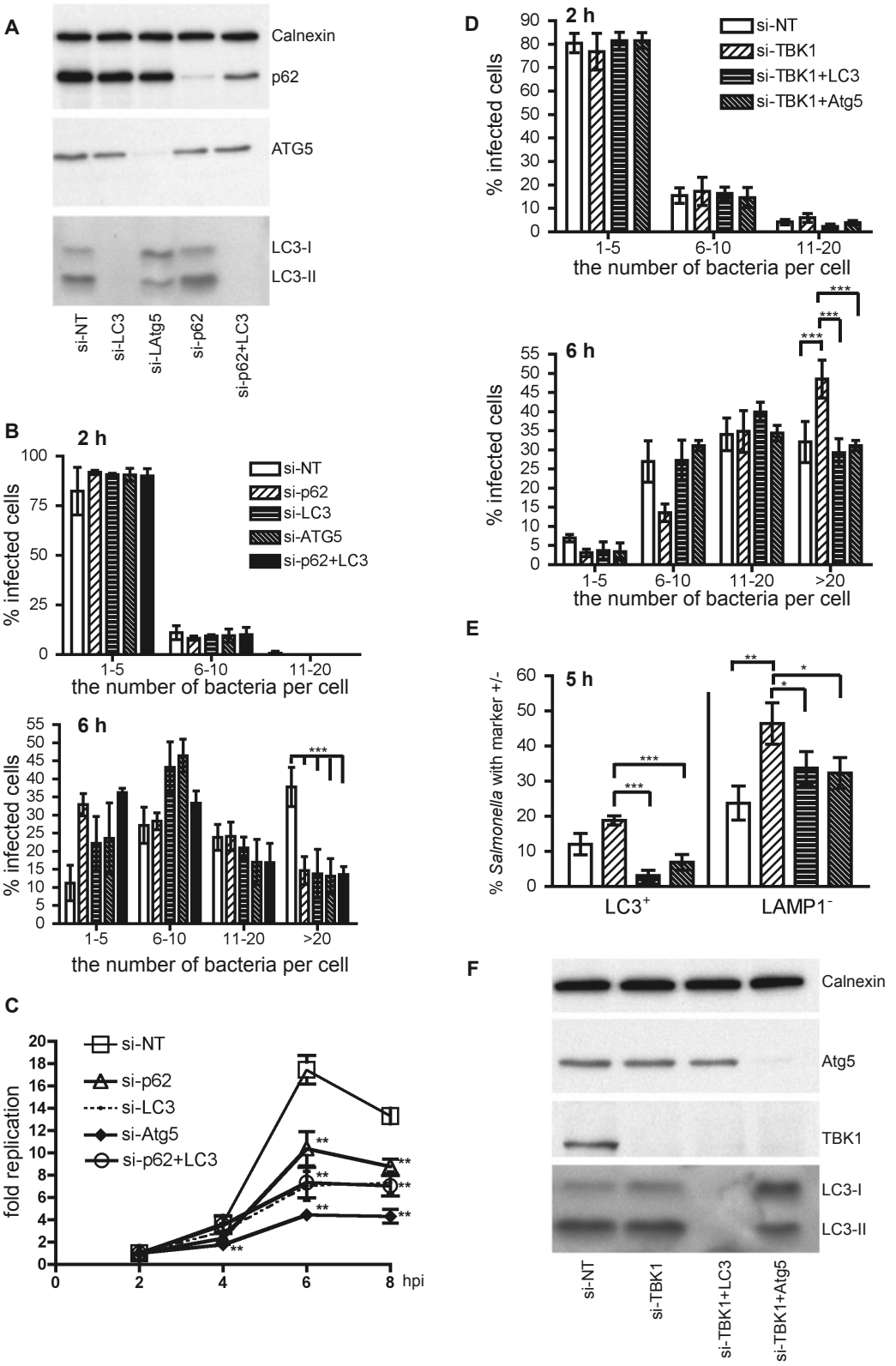

FIG 3 p62 and autophagy favors cytosolic replication of *Salmonella*. (A) Western blot analyses of HeLa cells treated with control siRNA (si-NT) or siRNA targeting p62 (si-p62), LC3 (si-LC3), Atg5 (si-Atg5), and p62 and LC3 (si-p62+LC3). These cells were infected with WT *Salmonella*. Calnexin was used as a loading control. (B) Microscopic analyses of infected cells containing 1 to 5, 6 to 10, 11 to 20, or greater than 20 bacteria per cell at 2 hpi (top) and 6 hpi (bottom). The number of bacteria in at least 50 infected cells was enumerated, and the percentage of cells containing the indicated number of bacteria was presented (mean ± SD, $n = 3$). (C) Replication of *Salmonella* was compared in HeLa cells used in panel A. The fold replication was calculated as fold increases of the number of

(Continued)

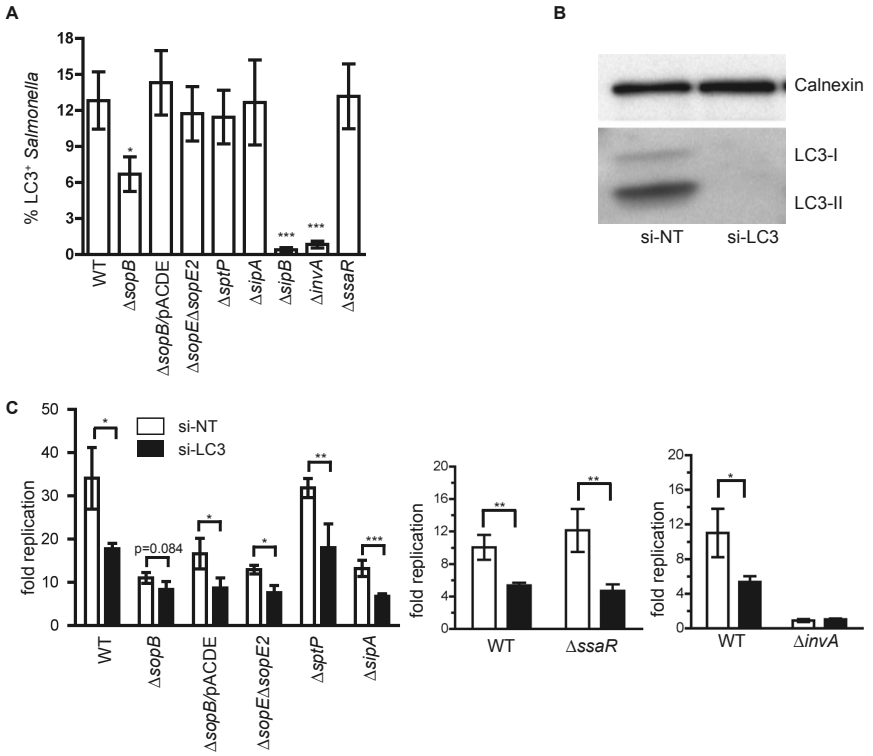

FIG 4 The effector SopB is required for *Salmonella* to associate with autophagosomes. (A) GFP-LC3-expressing cells were infected with the indicated strains. The Δ*sopB*/pACDE mutant expresses the wild-type SopB in a Δ*sopB* background. Unlike other strains that are individually used to infect cells, Δ*invA* and Δ*sipB* bacteria were used in a coinfection model. The percentage of $LC3^+$ bacteria at 5 hpi was quantified for each strain (mean ± SD, $n = 3$). (B) Western blot analysis of HeLa cells used in panel A. (C) HeLa cells treated with si-NT or si-LC3 were infected with the indicated strains. The fold replication of these strains at 6 hpi was determined (mean ± SD, $n = 3$).

the Δ*sopB* mutant was not as large as that observed for other mutants and the WT. Complementation of the Δ*sopB* mutant with a plasmid (pACDE) expressing SopB partially restored the replication of the Δ*sopB* mutant in control siRNA-treated cells but not in LC3 siRNA-treated cells. Thus, SopB is able to enhance *Salmonella* replication through increasing the interaction of *Salmonella* with autophagy. Unlike the WT and other mutants, Δ*invA* bacteria did not show a replication defect (or benefit) in LC3 siRNA-treated cells in a coinfection model (Fig. 4C, right). This suggests that even within the same cell, the replication/survival of the Δ*invA* mutant, but not the WT, is independent of autophagy.

Collectively, these data suggest that, together with the T3SS apparatus proteins InvA and SipB, the effector SopB is required for *Salmonella* to associate with autophagosomes for replication in HeLa cells.

Cells containing hyperreplicating bacteria and showing decreased autophagy are positive for caspase-1 and caspase-3/7 activation and undergo cell death. Cells containing hyperreplicating *Salmonella* can be extruded out of the epithelial monolayer and undergo cell death, releasing intracellular bacteria into the lumen that facilitate the dissemination of *Salmonella* to neighboring cells (5). Based on this concept, we tracked the fate of the hyperreplicating bacterium-containing (HRBC) cells. A real-time analysis of a *Salmonella*-infected GFP-LC3-expressing cell showed that a subset of *Salmonella* was hyperreplicating in the cytosol where it frequently associated with LC3 at 4.5 hpi (see Movies S1 and S5). The hyperreplication of *Salmonella* was accompanied by the decrease of LC3 levels in the cell at late time points. Such decreased LC3 signals correlated with lower levels of autophagosome formation (i.e., decreased autophagy), as bafilomycin (a drug used to block the fusion of autophagosomes with lysosomes) treatment did not increase LC3 signals in HRBC cells (data not shown). The decreased autophagy was observed in more than 90% of HRBC cells. As shown in Movie S5, the HRBC cell eventually detached from the plate. We speculated that the cell could be undergoing cell death, which led to its detachment from the plate. Consistent with this hypothesis, most (~86%) HRBC cells displaying decreased autophagy (as judged by the low level of p62 signals colocalized with *Salmonella*) showed abnormal (such as chromatin condensation and DNA fragmentation) nuclear mor-

Figure Legend Continued

bacteria at late time points compared to the number of bacteria at 2 hpi (mean ± SD, $n = 3$). (D) HeLa cells were treated with control siRNA (si-NT) or siRNA targeting TBK1 (TANK-binding kinase-1) (si-TBK1), TBK1 and LC3 (si-TBK1+LC3), and TBK1 and ATG5 (si-TBK1+ATG5) and infected with *Salmonella* for 2 h (top) or 6 h (bottom). The percentage of cells containing the indicated number of bacteria was quantified as in panel B (mean ± SD; $n = 3$). (E) GFP-LC3-expressing HeLa cells were treated with si-NT, si-TBK1, si-TBK1+LC3, or si-TBK1+Atg5. The percentage of $LC3^+$ bacteria or $LAMP\text{-}1^-$ bacteria at 5 hpi was quantified (mean ± SD, $n = 3$). (F) Western blot analyses of HeLa cells used in panel D.

phology at 8 hpi (Fig. 5A and B). In contrast, only ~33% of HRBC cells having normal autophagy (as judged by a relatively high level of p62 staining colocalized with *Salmonella*) contained abnormal nuclei (Fig. 5B). Figure 5C shows an HRBC cell with relatively enhanced autophagy exhibiting normal nuclear morphology.

We next sought to determine if HRBC cells with decreased autophagy were positive for active caspase-1 and caspase-3/7, both of which have been shown to be activated and capable of inducing cell death in extruding HRBC cells (5). As shown in Fig. 5D and E, HRBC cells with normal autophagy (as measured by the level of mRFP-LC3 associated with bacteria) and uninfected cells were negative for casapse-1 or caspase-3/7 staining, whereas the majority of HRBC cells with decreased autophagy were positive for active casapase-1 and caspase-3/7.

Taken together, these results suggest that hyperreplication of *Salmonella* accompanied by decreased autophagy and enhanced caspase-1 and caspase-3/7 activation promotes cell death, potentiating cell detachment at later stages of infection.

DISCUSSION

We propose that the p62-dependent autophagy pathway favors the replication of *Salmonella* in the cytosol of HeLa cells (Fig. 6). This concept is based on the following observations: (i) the increased association of p62 or LC3 with cytosolic *Salmonella* correlates with *Salmonella* replication; (ii) the replication of WT *Salmonella* and the Δ*sifA* mutant (a strain that escapes into the cytosol more often than the WT at 5 hpi) was reduced when p62, LC3, Atg5, or Atg16L1 was depleted; (iii) the replication of cytosolic *Salmonella* in TBK1 siRNA-treated cells (which increases the number of cytosolic bacteria) was reduced when autophagy was inhibited; (iv) p62 and LC3 belong to the same pathway to facilitate *Salmonella* replication; (v) most convincingly, live-cell imaging analyses demonstrated that a subset of cytosolic *Salmonella* associated extensively with p62 and/or LC3 and replicated quickly (in contrast, most intravacuolar *Salmonella* bacteria ineffectively associated with p62 and/or LC3 and replicated at much lower rates than cytosolic *Salmonella*); and (vi) hyperreplication of *Salmonella* in the cytosol concomitant with decreased autophagy and enhanced casapase-1 and caspase-3/7 activation potentiates cell death, leading to the detachment of HRBC cells at later times postinfection.

This model challenges the current dogma that p62 and autophagy protect host cells against *Salmonella* infection (16, 19, 29). The differing conclusions could be due to off-target effects of siRNA when used at high concentrations (~20 to 50 nM) by other groups as opposed to 1 nM in our study or incomplete dissociation of membrane-associated *Salmonella* when quantifying intracellular bacterial numbers. For instance, it is possible that the 0.1% Triton X-100 lysis buffer used in several seminal studies (14, 22, 30) dissociates autophagosome-associated *Salmonella* less efficiently than the 1% Triton X-100 and 0.1% SDS buffer used in this study. The time point at which bacteria were quantified may also be important. Zheng et al. (19) demonstrated that p62 limits *Salmonella* replication at 10 hpi, whereas we quantified bacteria at 6 hpi to avoid analysis when the host cells begin to detach or die at late time points (5). Additionally, the fate of autophagy-targeted *Salmonella* could be cell type dependent. In the first study examining the role of autophagy in *Salmonella* replication (16), Birmingham et al. examined the colocalization between autophagy markers and bacteria in HeLa cells and mouse embryonic fibroblasts (MEFs) but quantified only the effect of autophagy inhibition in MEFs. Thus, it is possible that inhibiting autophagy increases *Salmonella* replication in MEFs as they reported but has the opposite effect in HeLa cells, as we observed in this study.

Interestingly, Huang et al. recently showed that knockdown of Rab1, a GTPase required for autophagy of *Salmonella*, decreases *Salmonella* replication in HeLa cells (12). Although they interpreted this result as a distinct role for Rab1 in supporting *Salmonella* replication in vacuoles, a recent live-cell imaging study (17) convincingly shows that cytosolic replication of *Salmonella* accounts for the majority of the net replication of *Salmonella*. Thus, their observation with Rab1 knockdown could be explained by our model in which inhibiting autophagy reduces cytosolic *Salmonella* replication.

Autophagy also benefits several other bacterial pathogens, including *Legionella pneumophila*, *Coxiella burnetii*, and *Yersinia pseudotuberculosis* (29). Two mechanisms are proposed to contribute to the beneficial effects of autophagy on bacterial pathogens. First, through autophagolysosomal fusion, autophagosomes may serve as a source of nutrients for intracellular pathogens (7). This mechanism could partly explain why a previous study found that inhibition of autophagy by chloroquine (a drug that may block autophagolysosomal fusion, in addition to blocking acidification of the SCV) decreases *Salmonella* replication (31, 32). In support of this hypothesis, we were able to identify that oleic acid (a type of free fatty acid), but not amino acids, is likely to support *Salmonella* replication through autophagy (see Fig. S4A to C). However, the free fatty acid is not the limiting factor for *Salmonella* replication, since supplementation of the free fatty acid into autophagy-deficient cells does not rescue the replication defect of *Salmonella* (see Fig. S4C). There are likely other nutrients supplied by autophagy for *Salmonella* replication. Autophagosomes may also serve as a protected niche for intracellular pathogens (7). We speculate that before a complete fusion of the autophagosome and the lysosome, the autophagosome ensures *Salmonella* replication in a less acidic environment and/or accommodates replicating bacteria through constant membrane elongation. This hypothesis awaits further study.

In addition to confirming that *Salmonella* autophagy requires the SPI-1 T3SS, this study identifies that SipB is the key player mediating *Salmonella*-autophagosome association. Possibly through its pore-forming activity, SipB damages the SCV, allowing *Salmonella* to access the host cell cytosol where it can access the autophagy machinery. Alternatively, SipB translocated into the host cell cytosol induces the formation of autophagosomes (33), which in turn associate with ubiquitinated *Salmonella*. However, it is also possible that SipB functions as a translocon component to translocate other effectors that mediate *Salmonella*-autophagosome association. Unlike Δ*sipB* bacteria that were barely associated with autophagosomes, Δ*sopB* bacteria showed a moderately decreased association with autophagosomes, suggesting that SopB plays a lesser role than SipB in mediating *Salmonella*-autophagosome association. Since SopB can be ubiquitinated in host cells over a prolonged period (34), it will be interesting to determine if the ubiquitination of SopB enhances *Salmonella*-autophagosome association.

All together, our various cell biology-based assays, especially the live-cell imaging analyses, provide compelling evidence that *Salmonella* benefits from p62-dependent autophagy for its replication in the cytosol of HeLa cells.

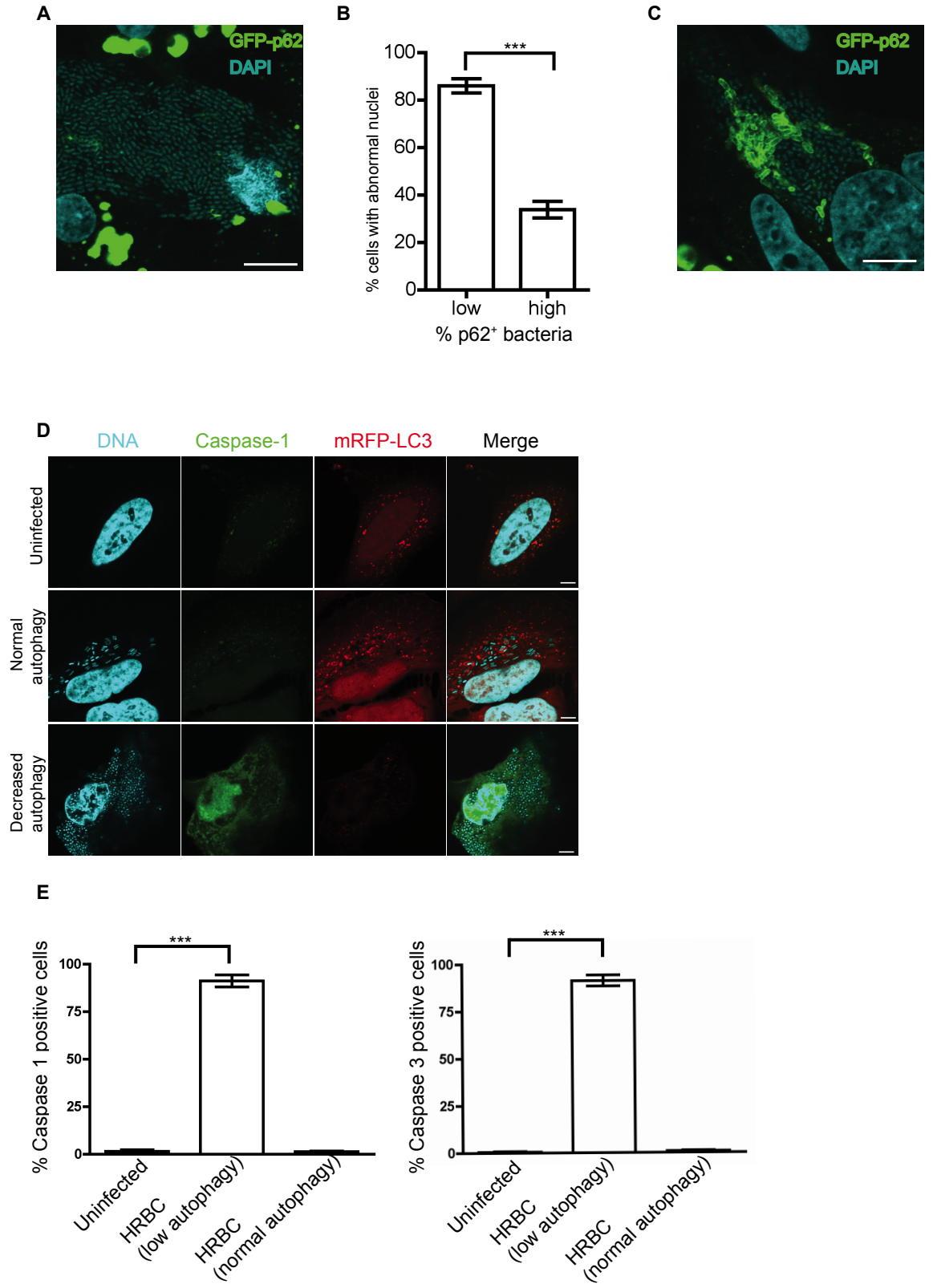

FIG 5 Cells containing hyperreplicating bacteria and showing decreased autophagy are positive for caspase-1 and caspase-3/7 activation and undergo cell death. (A) GFP-p62-expressing HeLa cells were infected with *Salmonella* for 8 h and stained with DAPI (blue). A cell containing hyperreplicating bacteria (more than 50 bacteria per cell, i.e., HRBC cells) and showing abnormal nuclear morphology is shown. Scale bar, 10 μm. (B) At least 100 HRBC cells were divided into two groups. The first group exhibited a low level of p62 signals colocalized with *Salmonella* (<1% of intracellular bacteria), and the second group exhibited a relatively high level of p62 signals (>2% of intracellular bacteria). The number of cells showing abnormal nuclear morphology (such as chromatin condensation and DNA

(Continued)

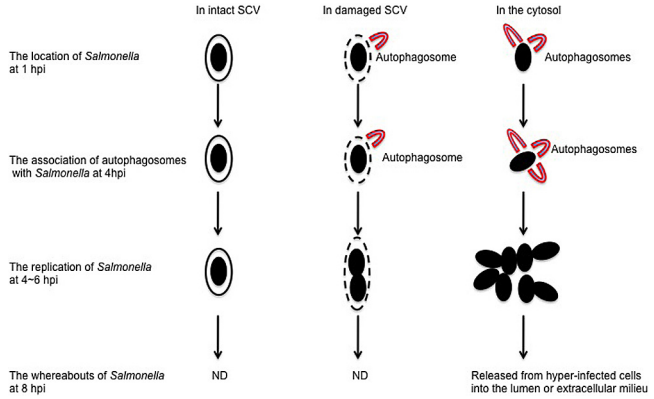

FIG 6 A proposed model for p62-dependent autophagy favoring *Salmonella* replication in the cytosol of HeLa cells. In this proposed model, *Salmonella* likely acquires nutrients supplied by autophagy for its replication. At least three populations of bacteria are present in infected HeLa cells. The first population of bacteria remains in intact *Salmonella*-containing vacuoles (SCVs). These bacteria replicate slowly, as they do not associate with autophagosomes and are difficult to acquire nutrients from the cytosol. The second population of bacteria is partially exposed to the cytosol through the gaps between damaged SCVs (16). These bacteria are ineffectively coated with ubiquitin and associated with autophagosomes to a low level. They acquire a limited amount of nutrients for replication and replicate faster than the first population of bacteria. The third population of bacteria is completely exposed to the cytosol. These bacteria are effectively coated with ubiquitin and associated with autophagosomes to a high level. They acquire sufficient nutrients from the cytosol and replicate the fastest. Notably, some cells containing the third population of bacteria will undergo cell death and detach from the epithelial layer, resulting in the release of hyperreplicating bacteria that are capable of initiating secondary infections in neighboring cells. The whereabouts of the first and second populations of bacteria at 8 hpi were not determined (ND).

MATERIALS AND METHODS

Bacterial strains and plasmids. Wild-type *Salmonella* (*Salmonella enterica* serovar Typhimurium strain SL1344) and its isogenic mutant strains were cultured as described previously (21). Details of various *Salmonella* strains and plasmids are summarized in Table S1 in the supplemental material.

Cell culture. HeLa human epithelial cells (ATCC CCL-2) and 293T/17 human kidney epithelial cells (ATCC CRL-11268) were maintained in Dulbecco's modified Eagle medium (DMEM) high glucose (Thermo Scientific) supplemented with 10% heat-inactivated fetal bovine serum (FBS), 1% nonessential amino acids (Invitrogen), and 1% GlutaMax (Gibco). Cells were used from passages 5 to 15.

Generation of stable cell lines with lentivirus infection. Lentivirus constructs pLVX-GFP-LC3^{WT}, pLVX-GFP, pLVX-GFP-p62, and pLVX-mRFP-LC3 were individually packaged into lentivirus particles in 293T/17 cells using the lentiviral packaging mix (Sigma). HeLa cells were infected with these lentivirus particles in the presence of 8 μg/ml Polybrene (Millipore) and selected in DMEM containing 3 μg/ml puromycin (Sigma) for 2 weeks. A single-cell-derived stable cell line was further obtained by culturing cells in a 96-well plate with a limiting dilution procedure.

Bacterial infection and gentamicin protection assay. *Salmonella* was cultured in Luria broth (LB) overnight at 37°C with shaking (200 rpm), followed by dilution into 10 ml of fresh LB (1:33), and continued to grow under the same conditions for 3 h. One milliliter of bacteria was then centrifuged at 8,000 × *g* for 2 min and resuspended in 1 ml of phosphate-buffered saline (PBS) containing Ca^{2+} and Mg^{2+} ($PBS^{+/+}$, pH 7.4). This suspension was diluted in DMEM (no antibiotics) at 1:500, and 335 μl of diluents was added directly to HeLa cells to give a multiplicity of infection (MOI) of 10. After 10 min of infection, the monolayers were washed three times in $PBS^{+/+}$ and then incubated in fresh culture medium. After 20 min, fresh culture medium containing 100 μg/ml gentamicin was added. At 2 hpi, the gentamicin concentration was reduced to 10 μg/ml. For coinfection experiments, wild-type *Salmonella* and mutant strains were mixed at a ratio of 1:40 before infection. At designated time points, cells were washed three times with PBS and lysed in 250 μl of lysis buffer (PBS with 1% Triton X-100 and 0.1% SDS). Bacteria released from cells were plated onto an LB agar plate (with 100 μg/ml streptomycin and 50 μg/ml kanamycin to select mutant strains) to obtain the bacterial CFU. The number of bacteria recovered at 2 hpi defines the invasion ability of *Salmonella*, whereas the fold increase of CFU at later time points versus the CFU at 2 hpi is referred to as fold replication and defines the replication ability of *Salmonella*.

Transient transfection with siRNA. All small interfering RNAs (siRNAs) are from a pool of four single siRNAs that targets the same gene (SMARTpool siRNA; Dharmacon RNA Technologies). The following siRNA SMARTpools (catalog no.) are used: p62 siRNA (M-010230-00), Atg5 siRNA (M-004374-04), Atg16L1 siRNA (M-021033-02), TBK1 siRNA (M-003788-02), LC3A siRNA (M-013579-00), LC3B siRNA (M-012846-01), LC3C siRNA (M-032399-01), and nontargeting scrambled control siRNA (D-001206-13). For LC3 knockdown, 1 nM of each LC3A, LC3B, and LC3C siRNA was used for transfection. One day before transfection with siRNA, HeLa cells were seeded at densities of 7.5×10^5 per 10-cm dish in 8 ml DMEM without antibiotics. Cells were transfected with 1 nM siRNA using INTERFERin (Polyplus Transfection) according to the manufacturer's instructions. One day after transfection with siRNAs, cells were trypsinized and seeded into a 24-well plate at a density of 4×10^4 cells per well. Bacterial infections were performed 48 h posttransfection.

Western blot analysis. Cells were washed three times with PBS and lysed in NP-40 buffer (20 mM Tris-HCl [pH 7.5], 150 mM NaCl, 1% [vol/vol] Nonidet P-40, 10 mM Na $_4P_2O_7$, 50 mM NaF) supplemented with a complete protease inhibitor tablet (Roche). The protein of interest was then detected by the standard immunoblotting method.

Antibodies and reagents. Antibodies used for Western blotting and immunofluorescence were anti-p62 (BD Transduction Laboratories), anti-LC3, anti-Atg16L1, and anti-ubiquitin (MBL International Incorporation), anti-Atg5 (Cell Signaling), anti-TBK1 (Imgenex), anti-FLAG and anti-calnexin (Sigma), anti-LAMP-1 (clone H4A3), and Alexa Fluor 488 and Alexa Fluor 568 (Invitrogen). Dimethyl sulfoxide (DMSO) and oleic acid (conjugated to albumin) were purchased from Sigma. Nonessential amino acids at the final concentration of 10× and essential amino acids at the final concentration of 5× (Invitrogen) were supplemented into the medium for 3 h before infection; oleic acid (200 μM) was added into the medium for 15 h before infection. All the above-named reagents remained in the medium throughout the subsequent infection.

Figure Legend Continued

fragmentation) was further quantified and expressed as the percentage of cells with abnormal nuclei in each group of cells (mean ± SD, $n = 3$). (C) A GFP-p62-expressing HRBC cell shows a relatively enhanced autophagy and normal nuclear morphology. Scale bar, 10 μm. (D) Cells stably expressing monomeric red fluorescent protein (mRFP)-LC3 were infected with WT *Salmonella* for 7 h and stained with DAPI (blue) and active caspase-1 probe FAM-YVAD-FMK (green) or caspase-3/7 probe FAM-DEVD-FMK (similar to caspase-1 staining [data not shown]). (E) Quantification of the percentage of casapase-1 (left)- or caspase-3/7 (right)-positive cells in uninfected cells, HRBC cells showing decreased autophagy, and HRBC cells showing normal autophagy at 8 hpi (mean ± SD, $n = 3$).

Cell viability assay. Equal volumes of cells (including floating cells in the medium) and 0.4% trypan blue (Invitrogen) were mixed and incubated at room temperature for 3 min. The stained cells were visualized by a bright-field microscope. The viable cell will exclude trypan blue and have a clear cytoplasm, whereas a nonviable cell will take up trypan blue and have a blue cytoplasm. At least 100 cells were counted and used to calculate the percentage of viable cells.

Immunofluorescence staining and fluorescence microscopy. Cells were fixed by 4% paraformaldehyde (PFA) for 30 min at room temperature, followed by washing with $PBS^{+/+}$ twice. Excess PFA was quenched by incubation of the cells with 50 mM NH_4Cl for 10 min. Fixed cells were blocked and permeabilized by incubation buffer (IB; $PBS^{+/+}$ containing 0.2% saponin, 10% normal goat serum) for 30 min. Permeabilized cells were sequentially incubated in IB containing primary (1 h) and secondary (1 h) antibody at room temperature. Coverslips that contain the cells were mounted on glass slides using ProLong Gold with 4′,6-diamidino-2-phenylindole (DAPI; Invitrogen) and sealed with nail polish.

All images are shown as representative confocal z-slices unless otherwise indicated. Images were taken with a multiphoton laser scanning microscope (Olympus FV1000MPE) operated by FV10-ASW software. Adobe Photoshop and Adobe Illustrator were used to process pictures exported from the FV10-ASW software. For quantification of bacteria associated with fluorescence signals, a Zeiss 510 metafluorescence microscope was used. For each condition, at least 100 bacteria or 50 infected cells were analyzed.

Live-cell imaging. Cells were cultured on glass-bottom dishes (MatTek). In most cases, unless otherwise indicated, cells were washed with PBS containing Ca^{2+} and Mg^{2+} (pH 7.4; $PBS^{+/+}$) twice at 2 hpi and imaged in Leibovitz's L-15 medium (Invitrogen) containing 10% FBS, Oxyrase (1:100) (Oxyrase), and 10 μg/ml gentamicin. Cells were imaged with a high-speed spinning-disc confocal microscope (PerkinElmer) at designated intervals. Images were acquired and analyzed with Volocity three-dimensional (3D) image analysis software (Improvision). Movies were exported from the Volocity software in QuickTime movie format and edited with the iMovie software if necessary.

Live-cell staining. One day before infection (MOI of 10), 1.5×10^5 cells were seeded into a 35-mm glass-bottom dish (MatTek). One hour before imaging, LysoTracker red (100 nM, Invitrogen) was added into the medium. Right before imaging with a spinning-disc confocal microscope, cells were washed with $PBS^{+/+}$ twice and replaced with Leibovitz's L-15 medium containing 10% FBS, Oxyrase (1:100), and 10 μg/ml gentamicin. To stain active caspase-1 or caspase-3/7, cells (at 7 hpi) grown on coverslips were incubated with FAM-YVAD-FMK or FAM-DEVD-FMK (Immunochemistry Technologies), respectively. One hour after the incubation, cells were further processed according to the instructions from the manufacturer and mounted on glass slides using ProLong Gold with DAPI.

Correlative light microscopy-electron microscopy (CLEM). HeLa cells stably expressing EGFP-LC3 were cultured on glass-bottom dishes and infected with *Salmonella* for 5 h. The samples were processed similarly to those performed by Kageyama et al. (35). A spinning-disc confocal microscope (PerkinElmer Ultraview VoX) was used to identify cells containing GFP-$LC3^+$ bacteria. A transmission electron microscope (Hitachi 7600) was used to take the electron micrographs of cells containing GFP-$LC3^+$ bacteria.

Statistical analysis. All analyses were performed with a 95% confidence interval using GraphPad Prism version 4.0, and the data were expressed as mean values ± standard deviations (SD). To calculate the *P* values, a two-tailed Student *t* test was used for Fig. 1B to D, 4C, 5B, and Fig. S1C, D, and G and S3D in the supplemental material; a one-way analysis of variance (ANOVA) with Dunnett's *post hoc* test was used for Fig. 3C and E, 4A, 5E, and Fig. S1E and S3A and C in the supplemental material; a two-way ANOVA with Bonferroni posttest was used for Fig. 3B and D and Fig. S4A to C in the supplemental material (*, $P < 0.05$; **, $P < 0.01$; ***, $P < 0.001$).

SUPPLEMENTAL MATERIAL

Supplemental material for this article may be found at http://mbio.asm.org/lookup/suppl/doi:10.1128/mBio.00865-14/-/DCSupplemental.

Figure S1, PDF file, 7.1 MB.
Figure S2, PDF file, 0.5 MB.
Figure S3, PDF file, 0.2 MB.
Figure S4, PDF file, 0.1 MB.
Table S1, DOC file, 0.1 MB.
Movie S1, MOV file, 4.4 MB.
Movie S2, MOV file, 2.6 MB.
Movie S3, MOV file, 3.3 MB.
Movie S4, MOV file, 1.8 MB.
Movie S5, MOV file, 3.2 MB.

ACKNOWLEDGMENTS

This work was supported by operating grants from the Canadian Institutes of Health Research (CIHR) (B.B.F. and L.J.F.), a postdoctoral fellowship from CIHR and Inimex Pharmaceuticals, Inc. (H.B.Y.), a postdoctoral fellowship from the CIHR (R.B.R.F.), a Canadian Association of gastroenterology/CIHR/Ferring Pharmaceuticals postdoctoral fellowship (M.A.C.).

B.B.F. is the University of British Columbia Peter Wall Distinguished Professor. L.J.F. is the Canada Research Chair in quantitative proteomics. No competing interests exist for this work.

We thank members of the Finlay lab for critical reading of the manuscript, T. Ratajczak for providing the plasmid pCDNA3-GFP-p62, and G. Martens, B. Ross, and K. Hodgson for technical help on immunofluorescence microscopy and electron microscopy.

REFERENCES

1. **Ohl ME, Miller SI.** 2001. *Salmonella*: a model for bacterial pathogenesis. Annu. Rev. Med. **52:**259–274. http://dx.doi.org/10.1146/annurev.med.52.1.259.
2. **Haraga A, Ohlson MB, Miller SI.** 2008. Salmonellae interplay with host cells. Nat. Rev. Microbiol. **6:**53–66. http://dx.doi.org/10.1038/nrmicro1788.
3. **Jones BD, Ghori N, Falkow S.** 1994. *Salmonella* Typhimurium initiates murine infection by penetrating and destroying the specialized epithelial M cells of the Peyer's patches. J. Exp. Med. **180:**15–23. http://dx.doi.org/10.1084/jem.180.1.15.
4. **Menendez A, Arena ET, Guttman JA, Thorson L, Vallance BA, Vogl W, Finlay BB.** 2009. *Salmonella* infection of gallbladder epithelial cells drives local inflammation and injury in a model of acute typhoid fever. J. Infect. Dis. **200:**1703–1713. http://dx.doi.org/10.1086/646608.
5. **Knodler LA, Vallance BA, Celli J, Winfree S, Hansen B, Montero M, Steele-Mortimer O.** 2010. Dissemination of invasive *Salmonella* via bacterial-induced extrusion of mucosal epithelia. Proc. Natl. Acad. Sci. U. S. A. **107:**17733–17738. http://dx.doi.org/10.1073/pnas.1006098107.
6. **Brumell JH, Tang P, Zaharik ML, Finlay BB.** 2002. Disruption of the *Salmonella*-containing vacuole leads to increased replication of *Salmonella enterica* serovar Typhimurium in the cytosol of epithelial cells. Infect. Immun. **70:**3264–3270. http://dx.doi.org/10.1128/IAI.70.6.3264-3270.2002.
7. **Levine B, Mizushima N, Virgin HW.** 2011. Autophagy in immunity and inflammation. Nature **469:**323–335. http://dx.doi.org/10.1038/nature09782.
8. **Kabeya Y, Mizushima N, Ueno T, Yamamoto A, Kirisako T, Noda T, Kominami E, Ohsumi Y, Yoshimori T.** 2000. LC3, a mammalian homologue of yeast Apg8p, is localized in autophagosome membranes after processing. EMBO J. **19:**5720–5728. http://dx.doi.org/10.1093/emboj/19.21.5720.
9. **Mizushima N, Yamamoto A, Hatano M, Kobayashi Y, Kabeya Y, Suzuki K, Tokuhisa T, Ohsumi Y, Yoshimori T.** 2001. Dissection of autophagosome formation using Apg5-deficient mouse embryonic stem cells. J. Cell Biol. **152:**657–668. http://dx.doi.org/10.1083/jcb.152.4.657.
10. **Deretic V.** 2010. Autophagy in infection. Curr. Opin. Cell Biol. **22:**252–262. http://dx.doi.org/10.1016/j.ceb.2009.12.009.
11. **Roy D, Liston DR, Idone VJ, Di A, Nelson DJ, Pujol C, Bliska JB, Chakrabarti S, Andrews NW.** 2004. A process for controlling intracellular

bacterial infections induced by membrane injury. Science **304:**1515–1518. http://dx.doi.org/10.1126/science.1098371.
12. **Huang J, Birmingham CL, Shahnazari S, Shiu J, Zheng YT, Smith AC, Campellone KG, Heo WD, Gruenheid S, Meyer T, Welch MD, Ktistakis NT, Kim PK, Klionsky DJ, Brumell JH.** 2011. Antibacterial autophagy occurs at PI(3)P-enriched domains of the endoplasmic reticulum and requires Rab1 GTPase. Autophagy **7:**17–26. http://dx.doi.org/10.4161/auto.7.1.13840.
13. **Birmingham CL, Brumell JH.** 2006. Autophagy recognizes intracellular *Salmonella enterica* serovar Typhimurium in damaged vacuoles. Autophagy **2:**156–158.
14. **Thurston TL, Ryzhakov G, Bloor S, von Muhlinen N, Randow F.** 2009. The TBK1 adaptor and autophagy receptor NDP52 restricts the proliferation of ubiquitin-coated bacteria. Nat. Immunol. **10:**1215–1221. http://dx.doi.org/10.1038/ni.1800.
15. **Wild P, Farhan H, McEwan DG, Wagner S, Rogov VV, Brady NR, Richter B, Korac J, Waidmann O, Choudhary C, Dötsch V, Bumann D, Dikic I.** 2011. Phosphorylation of the autophagy receptor optineurin restricts *Salmonella* growth. Science **333:**228–233. http://dx.doi.org/10.1126/science.1205405.
16. **Birmingham CL, Smith AC, Bakowski MA, Yoshimori T, Brumell JH.** 2006. Autophagy controls *Salmonella* infection in response to damage to the *Salmonella*-containing vacuole. J. Biol. Chem. **281:**11374–11383. http://dx.doi.org/10.1074/jbc.M509157200.
17. **Malik-Kale P, Winfree S, Steele-Mortimer O.** 2012. The bimodal lifestyle of intracellular *Salmonella* in epithelial cells: replication in the cytosol obscures defects in vacuolar replication. PLoS One **7:**e38732. http://dx.doi.org/10.1371/journal.pone.0038732.
18. **Beuzón CR, Méresse S, Unsworth KE, Ruíz-Albert J, Garvis S, Waterman SR, Ryder TA, Boucrot E, Holden DW.** 2000. *Salmonella* maintains the integrity of its intracellular vacuole through the action of SifA. EMBO J. **19:**3235–3249. http://dx.doi.org/10.1093/emboj/19.13.3235.
19. **Zheng YT, Shahnazari S, Brech A, Lamark T, Johansen T, Brumell JH.** 2009. The adaptor protein p62/SQSTM1 targets invading bacteria to the autophagy pathway. J. Immunol. **183:**5909–5916. http://dx.doi.org/10.4049/jimmunol.0900441.
20. **Perrin AJ, Jiang X, Birmingham CL, So NS, Brumell JH.** 2004. Recognition of bacteria in the cytosol of mammalian cells by the ubiquitin system. Curr. Biol. **14:**806–811. http://dx.doi.org/10.1016/j.cub.2004.09.022.
21. **Steele-Mortimer O, Brumell JH, Knodler LA, Méresse S, Lopez A, Finlay BB.** 2002. The invasion-associated type III secretion system of *Salmonella enterica* serovar Typhimurium is necessary for intracellular proliferation and vacuole biogenesis in epithelial cells. Cell. Microbiol. **4:**43–54. http://dx.doi.org/10.1046/j.1462-5822.2002.00170.x.
22. **von Muhlinen N, Akutsu M, Ravenhill BJ, Foeglein A, Bloor S, Rutherford TJ, Freund SM, Komander D, Randow F.** 2012. LC3C, bound selectively by a noncanonical LIR motif in NDP52, is required for antibacterial autophagy. Mol. Cell **48:**329–342. http://dx.doi.org/10.1016/j.molcel.2012.08.024.
23. **Mizushima N, Kuma A, Kobayashi Y, Yamamoto A, Matsubae M, Takao T, Natsume T, Ohsumi Y, Yoshimori T.** 2003. Mouse Apg16L, a novel WD-repeat protein, targets to the autophagic isolation membrane with the Apg12-Apg5 conjugate. J. Cell Sci. **116:**1679–1688. http://dx.doi.org/10.1242/jcs.00381.
24. **Radtke AL, Delbridge LM, Balachandran S, Barber GN, O'Riordan MX.** 2007. TBK1 protects vacuolar integrity during intracellular bacterial infection. PLoS Pathog. **3:**e29. http://dx.doi.org/10.1371/journal.ppat.0030029.
25. **Collazo CM, Galán JE.** 1997. The invasion-associated type III system of *Salmonella* Typhimurium directs the translocation of Sip proteins into the host cell. Mol. Microbiol. **24:**747–756. http://dx.doi.org/10.1046/j.1365-2958.1997.3781740.x.
26. **Brumell JH, Rosenberger CM, Gotto GT, Marcus SL, Finlay BB.** 2001. SifA permits survival and replication of *Salmonella* Typhimurium in murine macrophages. Cell. Microbiol. **3:**75–84. http://dx.doi.org/10.1046/j.1462-5822.2001.00087.x.
27. **Ibarra JA, Steele-Mortimer O.** 2009. *Salmonella*—the ultimate insider. *Salmonella* virulence factors that modulate intracellular survival. Cell. Microbiol. **11:**1579–1586. http://dx.doi.org/10.1111/j.1462-5822.2009.01368.x.
28. **Zhou D, Chen LM, Hernandez L, Shears SB, Galán JE.** 2001. A *Salmonella* inositol polyphosphatase acts in conjunction with other bacterial effectors to promote host cell actin cytoskeleton rearrangements and bacterial internalization. Mol. Microbiol. **39:**248–259. http://dx.doi.org/10.1046/j.1365-2958.2001.02230.x.
29. **Mostowy S, Cossart P.** 2012. Bacterial autophagy: restriction or promotion of bacterial replication? Trends Cell Biol. **22:**283–291. http://dx.doi.org/10.1016/j.tcb.2012.03.006.
30. **Thurston TL, Wandel MP, von Muhlinen N, Foeglein A, Randow F.** 2012. Galectin 8 targets damaged vesicles for autophagy to defend cells against bacterial invasion. Nature **482:**414–418.
31. **Garcia-del Portillo F, Zwick MB, Leung KY, Finlay BB.** 1993. *Salmonella* induces the formation of filamentous structures containing lysosomal membrane glycoproteins in epithelial cells. Proc. Natl. Acad. Sci. U. S. A. **90:**10544–10548. http://dx.doi.org/10.1073/pnas.90.22.10544.
32. **Rubinsztein DC, Gestwicki JE, Murphy LO, Klionsky DJ.** 2007. Potential therapeutic applications of autophagy. Nat. Rev. Drug Discov. **6:**304–312. http://dx.doi.org/10.1038/nrd2272.
33. **Hernandez LD, Pypaert M, Flavell RA, Galán JE.** 2003. A *Salmonella* protein causes macrophage cell death by inducing autophagy. J. Cell Biol. **163:**1123–1131. http://dx.doi.org/10.1083/jcb.200309161.
34. **Patel JC, Hueffer K, Lam TT, Galán JE.** 2009. Diversification of a *Salmonella* virulence protein function by ubiquitin-dependent differential localization. Cell **137:**283–294. http://dx.doi.org/10.1016/j.cell.2009.01.056.
35. **Kageyama S, Omori H, Saitoh T, Sone T, Guan JL, Akira S, Imamoto F, Noda T, Yoshimori T.** 2011. The LC3 recruitment mechanism is separate from Atg9L1-dependent membrane formation in the autophagic response against *Salmonella*. Mol. Biol. Cell **22:**2290–2300. http://dx.doi.org/10.1091/mbc.E10-11-0893.